



Experimental investigation of a bubble column humidifier heated through solar energy

Fahad A. Al-Sulaiman^{a,b,*}, Hafiz M. Abd-ur-Rehman^{a,c}, Mohamed A. Antar^a,
Obaidallah Munteshari^a

^aMechanical Engineering Department, King Fahd University of Petroleum and Minerals, (KFUPM), Dhahran, 31261, Saudi Arabia, Tel. +966 13 860-4628; emails: fahadas@kfupm.edu.sa (F.A. Al-Sulaiman), abd-ur-rehman_@hotmail.com

(H.M. Abd-ur-Rehman), antar@kfupm.edu.sa (M.A. Antar), obaidallah@kfupm.edu.sa (Obaidallah Munteshari)

^bCenter of Research Excellence in Renewable Energy, King Fahd University of Petroleum and Minerals, (KFUPM), Dhahran, 31261, Saudi Arabia

^cSchool of Mechanical and Manufacturing Engineering (SMME), National University of Sciences & Technology (NUST), H-12 Campus, Islamabad, Pakistan

Received 24 January 2016; Accepted 25 July 2016

ABSTRACT

An experimental study was carried out to assess the performance of a novel bubble column humidifier operated through solar thermal energy. Different perforated plate geometries were studied experimentally to select the optimum design that delivers a low overall pressure drop in the system. Then, the day-round performance of the humidifier was investigated experimentally with and without Fresnel lens. The influence of the air superficial velocity, inlet water temperature, and inlet air relative humidity on the performance of the humidifier were investigated. Findings indicate that the average daily absolute humidity of the air at the exit of the humidifier increased by 12.3% when the air superficial velocity increased from 20 to 30 cm s⁻¹. This absolute humidity is further increased in the range of 9%–11% with the integration of the Fresnel lens. The new humidifier design can have a direct concentrated solar thermal heating and it acts as a heater for the water and air at the same time. Subsequently, it has high performance and it can be located in remote areas.

Keywords: Solar thermal energy; Water desalination; HDH systems; Bubble column humidifier; Fresnel lens; Air humidification

1. Introduction

The fresh water scarcity, energy crisis, and climate change are the most intimidating concerns for mankind as it brought many disquiets like health, pollution, and environmental issues [1]. The problem is more severe in developing countries where the population growth projection is much higher as compared with developed countries. The increase in world population growth results in a high demand for potable water that is well below the existing supply of fresh water. While the fresh water demand is rising exponentially,

the industrial revolution is making the fresh water scarcity situation more alarming by polluting the lakes and rivers by industrial waste. Given the fact that the population on earth continues to increase and industrial growth shows no signs of slowing down, it is inevitable that conventional sources of fresh water are not sufficient. To alleviate this threatening drift and the apprehensions of the existing and approaching fresh water crisis, the answer for water sustainability may lie in seawater desalination.

The process of seawater desalination is a mature expertise and is being adopted by many countries to yield potable water. These conventional process of water desalination are highly energy intensive [2] and economically suited only

* Corresponding author.

on large scale [3]. Moreover, the sustainability concerns of conventional energy sources and anxieties of climate change are making the present seawater desalination approaches unfavorable. Therefore, the use of renewable energy in seawater desalination is the only potential solution to balance the potable water requirements by secure and affordable energy with the pressing issue of climate change [4].

Solar energy is an appropriate energy choice for seawater desalination, but it is not economically viable for large scale conventional seawater desalination systems [5]. However, the use of solar energy is a promising option for developing a small scale water desalination systems for decentralized supply of fresh water in remote areas [6]. Solar humidification-dehumidification (HDH) is a carrier gas based thermal technique [7] that is ideal for decentralized small scale water desalination system [8] especially in remote regions where inexpensive land and abundant solar irradiance are available. The challenge is to come up with an efficient, reliable, and cost effective design approach to explore the true potential of the HDH water desalination systems. Several studies are available that explore HDH as an effective mean of brackish water desalination. However, the main focus of these studies is to improve the dehumidification process of the HDH system and comparatively less attention has been given toward the improvement of the humidification process.

Humidification is one of the fundamental processes in the solar HDH water desalination system. There are many devices, which can be used for the humidification purpose. These devices include spray tower, wetted wall tower, packed bed tower, and bubble column [9]. The aim of all these devices is to raise the humidity of the air by diffusion of water into unsaturated air stream. This diffusion phenomena is caused by the concentration variance between the water vapor in the air and air-water interface.

Several studies considered using spray tower as a humidification device in their HDH systems. In the spray tower, water is sprayed in the form of droplets that falls under the force of gravity. Air is injected from the bottom to come in a direct contact with the falling water droplets in a counter flow arrangement. These type of devices have low humidification effectiveness due to the low water holdup. Other limitations include the use of mist eliminators which are essential to avoid the water entrainment in the air at the exit of the spray tower. Furthermore, the losses in the spray nozzles causes a high pressure drop in the water stream. Wetted wall towers could also be used in an HDH system for air humidification purpose. In this configuration, thin water film flows downward on the inner perimeter to form a wetted surface along the tower length. The air stream can either flow upward or downward to have a direct contact with the falling water thin film. These towers have a higher humidification efficiency and a lower air-side pressure drop compared with other humidification towers. However, the water flow rate is restricted to a lower capacity because the thin film of water flows only on the inner perimeter of the tower. The packed bed tower is a widely practiced humidification device in the HDH water desalination system owing to its high performance. It is similar to the spray towers in which water is sprayed in the form of droplets that fall under the force of gravity. However, in the packed bed tower, the packing material is used to improve

the humidification efficiency. The use of a packing material makes the water droplets more dispersed which increases the area and time of contact between both water and air. However, this improvement leads to a higher pressure drop in the packed bed humidifier.

1.1. Bubble column humidification

An innovative design approach is to use the bubble column as a humidification device for an HDH water desalination system. In the humidifier configuration, air is passed through perforated plates to form bubbles in the hot water column. As the air bubbles propagate through the hot water column, simultaneous heat and mass transfer take place where air becomes hot and humid at the outlet of the humidifier. The higher rate of heat and mass transfer in a bubble column inspired the researchers to extensively use these devices as multiphase reactor in chemical process like fisher-tropsch process, in metallurgical and many biomedical applications [10]. However, the use of bubble column humidifier in HDH water desalination is very limited and there are very few studies that investigate the bubble column humidifier for HDH water desalination system. El-Agouz and Abugderah [11] carried out an experimental investigation of a single stage bubble column humidifier. An evaporator column of 500×250 mm cross section was used in this experiment. The air stream is introduced by a 75 mm diameter PVC pipe having 32 holes of 10 mm diameter on both sides. The pipe was submerged in the water and acted as a sparger to form bubbles in the pool of water. The efficiency of the humidifier is defined in terms of absolute humidity of the air at the inlet and exit state of the humidifier. The effect of water inlet temperature, the air inlet temperature, and the air inlet velocity on the humidifier efficiency was investigated. Their results indicated that the performance of the bubble column humidifier is considerably affected by the air inlet velocity and the water inlet temperature. The air inlet temperature has a slight influence on the air vapor contents difference. The highest efficiency achieved for the bubble column humidifier was reported as 95% with $222 \text{ g}_w \text{ kg}_a^{-1}$ at 75°C of air and water temperatures. Geometrical features, such as the number of holes, holes diameter, open area ratio, and water column height were not considered in this study. El-Agouz [12,13] performed another experimental study to analyze the effect of water column height, water column temperature, and air flow rate on the performance of bubble column humidifier. The effect of water column height on the efficiency of the bubble column humidifier was not significant. However, the performance of bubble column humidifier was increased with the increase in the water column temperature and air flow rate. The maximum efficiency achieved for the bubble column humidifier was reported as 98% at air flow rate of 14 kg h^{-1} and water temperature of 85°C .

Zhang et al. [14] studied experimentally the operating factors that affect bubbling humidification by using a single sieve plate. The result showed that the air relative humidity reached to 100%. Moreover, humidification capacity was increased by about 80% when water temperature was increased by 10°C . Zhang et al. [15] performed another experimental study on a single stage bubble column

humidifier to analyze the effect of air flow rate and water level on the pressure drop and the relative humidity of air. A cylindrical column of 198 mm diameter was used as an evaporator chamber in their experiment. A sieve plate of 8 mm thickness having 91 holes of 1 mm diameter was used as a sparger. Their experimental work aimed to achieve a high water vapor concentration in the air at the exit of the humidifier with a less pressure drop and a low blower power consumption. The results showed that the increase in the water level and air flow rate caused a greater pressure drop and a higher blower energy consumption. The moisture contents at the exit of the humidifier were increased with the increase of the water and air temperatures. In the range of experimental operating conditions, the experimental results showed that the air reached almost 100% relative humidity.

In all the aforementioned experimental investigation of the bubble column humidifier, water is heated by an electric heater that limits the use of these devices in remote areas where electricity availability is scarce. Therefore, a novel bubble column humidifier is proposed that is operated through solar thermal energy as the main source of energy input. In this humidifier, the absorber plate and bubble column were incorporated in a single frame design, as shown in Fig. 1. The absorber plate is tilted to an angle equal to the latitude of Dhahran (26.3°), Saudi Arabia to absorb the maximum

solar irradiance. This design improvement has the following advantages:

- The tilted absorber plate acts as a sloped surface to create a thin film of water over the absorber plate. The minimum water depth over the absorber plate leads to a better heat transfer and a higher water temperature is achieved at the downstream of absorber plate. It also results in a significantly low pressure drop in the air-side.
- The hot humid air at the exit of the bubble column further passed over the thin film of hot water flowing over absorber plate to absorb more moisture and higher vapor contents are achieved at the exit of humidifier. In other words, the humidifier heats both air and water simultaneously and air humidification process occurs throughout the full path of the air inside the humidifier.
- This proposed humidifier have a direct solar thermal heating. Subsequently, it can be located in remote areas, where there is a shortage in electricity.

The overall objective of this work is to develop and test the proposed humidifier design to identify the optimum operating conditions for possible integration with a dehumidifier. Consequently, an improved HDH performance design is obtained.

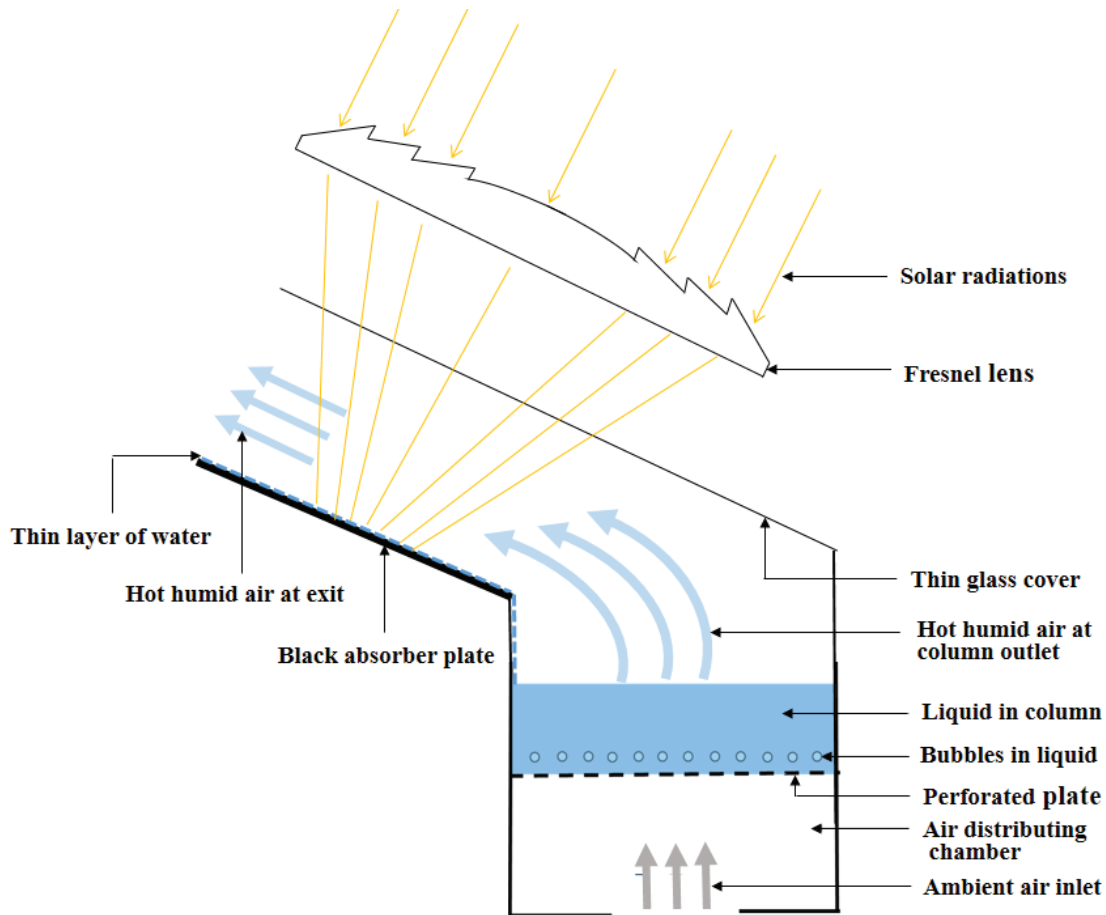


Fig. 1. Design of bubble column humidifier.

2. Experimental setup

A laboratory scale setup for the bubble column humidifier is designed and built as shown in Fig. 2. The frame of the experimental setup was constructed of 10 mm thick Plexiglas sheet. Plexiglas is a transparent thermoplastic material that has a thermal conductivity of 0.19 W m.K^{-1} . Furthermore, the use of such transparent material is advantageous in a sense that it allows the observer to see what is happening inside the unit while performing the experiment. Another advantage of using the Plexiglas is its low thermal conductivity that reduces the heat losses from the system. Plexiglas sheets are also used to build the bubble column of $300 \times 300 \text{ mm}$ cross section and 400 mm height. A perforated plate is used as a sparger to form the bubbles in a pool of hot water in the bubble column. The perforated plate is made of a 2 mm thick black acrylic Plexiglas. The perforated plate splits the bubble

column into lower and upper compartments. Air is introduced by a 400 W adjustable blower to the lower compartment of the bubble column through a 25 mm diameter CPVC pipe. The lower compartment of the bubble column is 300 mm high. It is used to distribute the air stream uniformly through the perforated plate. The upper compartment of the bubble column is 100 mm high. It is used as a pool for hot water that is down streamed from the absorber plate. The absorber plate is $300 \times 800 \text{ mm}$ in cross section and made of a 3 mm thick stainless steel. A Fresnel lens of 1 m^2 area is placed at the top of absorber plate. The Fresnel lens provide the geometric concentration ratio of approximately 4 and help in achieving the higher temperature at the downstream of absorber plate. The cover of the humidifier is made of 2 mm thin transparent glass to ensure maximum transmittance of solar irradiance. The reason for not using the Plexiglas sheet as a cover is its comparatively lower transmittance that further decreases

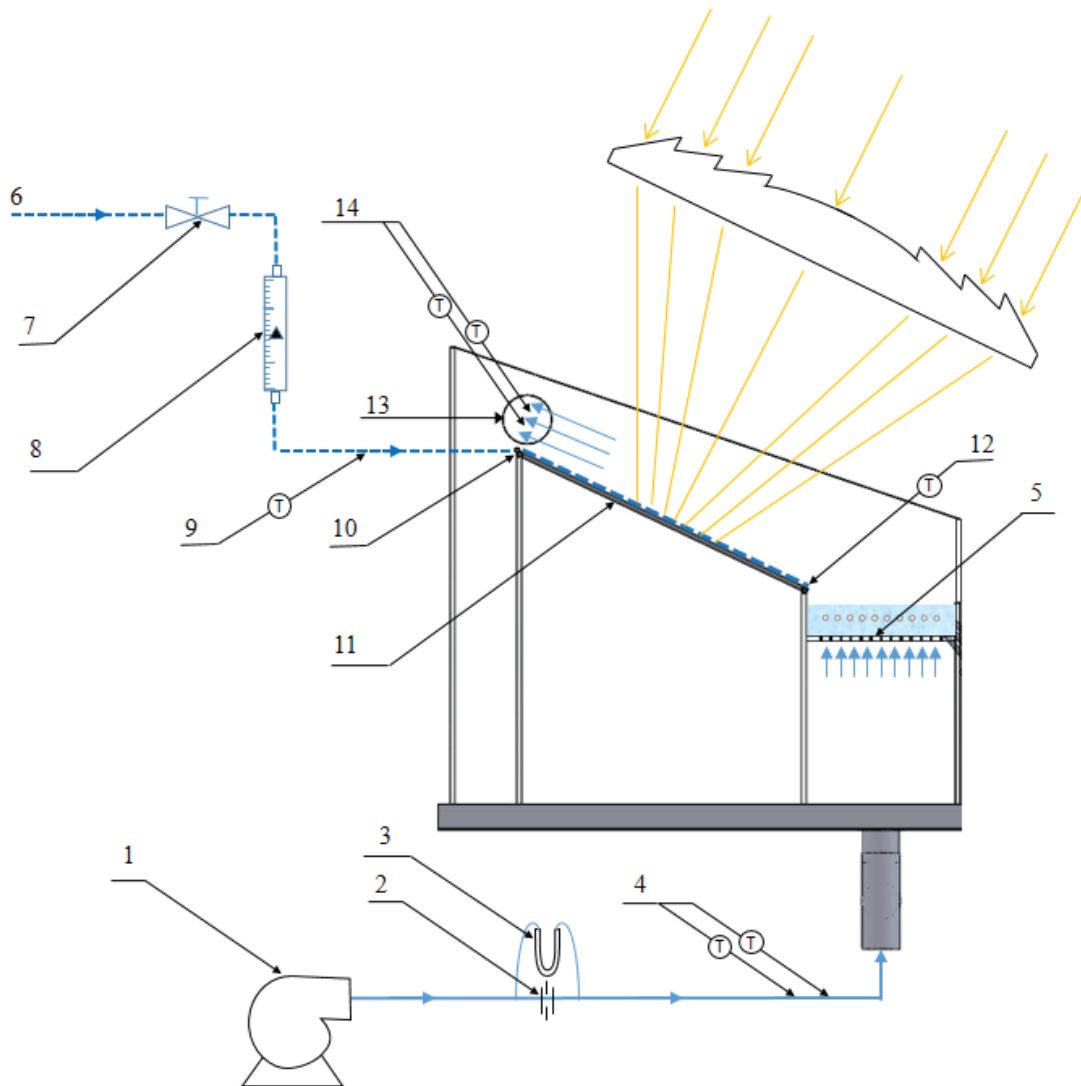


Fig. 2. Schematic diagram of experimental setup. (1) Air blower; (2) Orifice meter;(3) Manometer; (4, 9, 12, 14) Thermocouple; (5) Perforated plate;(6) Water supply;(7) Throttle valve;(8) Rotameter;(10) Water inlet; (11) Absorber plate, (13) Air outlet.

with the passage of time as the Plexiglas loss its clarity and adopt the yellowish color.

The experiment starts by blowing air using the air blower (1). The reason for blowing air first is that if the water flows first, it will penetrate down through the perforated plates (5). The blower is adjustable for the desired volumetric flow rate of the air stream that is measured by an orifice meter (2) connected to a manometer (3) to measure the pressure drop across the orifice plate and hence calculate air flow rate. The air dry-bulb/wet-bulb temperatures are measured by K-type thermocouples (4) before the air stream is admitted into the humidifier. Water supply (6) valve is then opened. The volumetric flow rate of the water is measured by a rotameter (8) adjusted to the desired value by a throttle valve (7). Water temperature is measured by a thermocouple (9) before entering the humidifier (10). A water film is distributed evenly over the black absorber plate (11) and flows by gravity. Water temperature increases as it flows over the absorber plate that is heated by solar irradiance. Water temperature is measured at the exit of the absorber plate using thermocouples (12). Hot water then moves to the bubble column chamber where air is passed through the perforated plate to form bubbles in the pool of the hot water. As the air bubbles propagate through the hot water column, simultaneous heat and mass transfer take place such that air is heated and humidified till it reaches the exit of the humidifier (13). Dry-bulb/wet-bulb temperatures of the hot and humid air are recorded using thermocouples (14) at the exit of the humidifier.

A data acquisition consisting of two NI 9213 thermocouple input modules installed in a NI cDAQ-9178 USB chassis is connected to a computer. Thermocouples measurements are displayed and stored using a Labview program. Real-time processed thermocouple readings are measured every 2 s and the average temperatures of every 5 min were recorded using the developed Labview program.

The air absolute humidity is measured by the psychometric calculations of the dry-bulb/wet-bulb temperatures at different locations in the humidifier. The difference of air absolute humidity between the outlet and inlet state of the humidifier provided the vapor content difference achieved by the air in the humidifier. The ratio of actual vapor content difference to maximum vapor content difference defined the humidification efficiency of the humidifier and is calculated as:

$$\text{Humidification efficiency} = \frac{\omega_{\text{out}} - \omega_{\text{in}}}{\omega_{\text{out}}^{\text{sat}} - \omega_{\text{in}}} \quad (1)$$

where ω_{out} is the absolute humidity of the air at the exit of the humidifier; ω_{in} is the absolute humidity of the air at the inlet of the humidifier; and $\omega_{\text{out}}^{\text{sat}}$ is the saturated absolute humidity of the air at the outlet of the humidifier.

In all the experimental investigations of the bubble column humidifier, the humidification efficiency was evaluated by using Eq. (1). As the core objective of the direct contact humidifier is to attain higher vapor contents in the moist air at the outlet, the efficiency of the humidifier can be represented in terms of humidity difference of the moist air between its inlet and outlet states. However, this approach is not appropriate to analyze the performance of a solar humidifier as it

does not take into account the effective utilization of solar energy by the humidifier. Therefore, another performance metric that relates the amount of energy added to the air stream to the solar energy incident on the humidifier is used to analyze the performance of the system. This performance metric is named as solar humidification efficiency and defined as:

$$\text{Solar humidification efficiency} = \frac{\dot{m}_{a,o} h_{a,o} - \dot{m}_{a,i} h_{a,i}}{Q_{\text{solar}}} \quad (2)$$

where Q_{solar} is the amount of solar energy incident on the humidifier and h_a is the specific enthalpy of moist air that includes the enthalpy of dry air (sensible heat) and the enthalpy of evaporated water in the air (latent heat). The specific enthalpy h_a is calculated as:

$$h_a = h_{da} + x h_{wv} \quad (3)$$

where x is the humidity ratio expressed as the ratio between the actual mass of water vapor present in moist air to the mass of the dry air, h_{da} is the specific enthalpy of the dry air (sensible heat), and h_{wv} is the specific enthalpy of the water vapors (latent heat). The specific enthalpy of dry air and water vapor is calculated by Eqs. (4) and (5), respectively.

$$h_{da} = c_{p,da} T_a \quad (4)$$

$$h_{wv} = c_{p,wv} T_w + h_{e,w} \quad (5)$$

where c_p is the specific heat, T is the temperature, and h_e is evaporation heat.

K-type thermocouples are used to measure water temperature as well as air dry-bulb/wet-bulb temperatures. Thermocouple probes are calibrated before installing them in the experimental setup. The volumetric flow rate of the water is measured by using FL5000 series rotameter of OMEGA. The volumetric flow rate of the air is measured by an orifice meter connected to a manometer to read the pressure drop across the orifice plate. The orifice meter is designed and installed according to the ISO 5167 benchmark design recommendations. Solar radiation is measured using a hand-held pyranometer. The uncertainty in the measurements is calculated as the root sum square of the fixed error of the instrumentation and the random error observed during different measurements [16]. The measurement devices along with their range, accuracy, and uncertainty are summarized in Table 1.

3. Results and discussion

3.1. Influence of geometry of the perforated plate

The optimum design consideration of the perforated plate is an important aspect in the experimental investigation of the bubble column humidifier. In the design of the perforated plate, the perforations geometric configuration should be optimized to reduce air pressure drop. Another important aspect in the perforated design is to avoid water leakage through the perforations. Keeping in mind the aforementioned aspects, three different perforated plates were

Table 1
Measurement devices along with their range, accuracy, and uncertainty

Properties	Instruments	Range	Accuracy	Uncertainty
Temperature	NI cDAQ-9178,	-267°C – 316°C	± 0.1°C	± 0.25°C
Relative humidity	K-Type thermocouple	0% – 100% RH	± 0.1% RH	± 0.93%
Pressure	U-Tube manometer	0.1 – 50 cm H ₂ O	± 1 mm	± 0.1 cm H ₂ O
Water flow rate	Rotameter	1 – 7 LPM	± 5% of full scale	± 0.2 LPM
Water column height	Graduate level	0.1 – 20 cm	± 1 mm	± 0.25 cm
Air superficial velocity	Orifice meter	10 – 50 cm s ⁻¹	± 1 cm s ⁻¹	± 0.79 cm s ⁻¹
Solar irradiance	Pyranometer	0–2,000 W m ⁻²	± 5% of full scale	± 1 W m ⁻²

Table 2
Geometric features of different designs of perforated plate tested during experimentation

	Number of holes	Hole diameter (mm)	Pitch size (mm)	Open area ratio (%)
Design 1	105	3	25	0.77
Design 2	105	2	25	0.33
Design 3	149	2	20	0.49

designed and tested to analyze the effect of perforation geometry on the performance of the bubble column humidifier. The geometric features of the three spargers used during the experimental work are listed in Table 2.

The open area ratio of the perforated plate is defined as the ratio of the perforation area to the plate area. The three different designs of perforated plates with different open area ratio were tested at different air superficial velocities. Results are shown in Fig. 3.

The minimum pressure drop is achieved using design 1 due to bigger hole diameter and higher open area ratio compared with the other two designs. However, water leakage was observed from the perforations during the experiments that showed that this design is not useful. To overcome the problem of the water leakage, design 2 was tested with the same number of holes as in design 1, that is, 105 holes; but the hole diameter was reduced from 3 to 2 mm. Design 2 was successful in preventing water leakage from the perforations but the pressure drop was high. The high pressure drop is due to the low open area ratio in design 2. Therefore, design 3 was tested with 149 holes with 2 mm hole diameter. The higher number of holes increased the open area ratio and reduced the pressure drop compared with design 2. Moreover, no leakage was observed with design 3 during the experiment. Therefore, design 3 was selected as the best choice for our experimental setup. The perforated plate dimensions and hole geometry of design 3 are shown in Fig. 4. The perforated plate is 300 × 300 mm in cross section and it consists of 149 holes, 2 mm-diameter each. The holes are made in equilateral triangular configuration where the distance between any two adjacent holes is 20 mm. The holes are distributed 40 mm away from the boundary of the perforated plate to avoid the shear stresses near the wall of the bubble column.

Experiments are performed to find out the effect of water column height on the total air pressure drop at different air

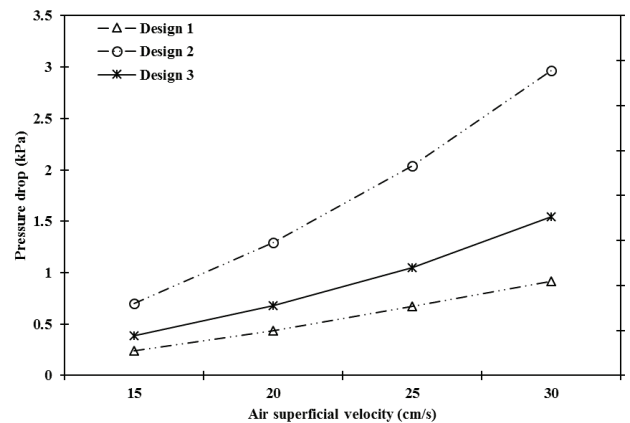


Fig. 3. Influence of air superficial velocity on the pressure drop under different design considerations of perforated plate.

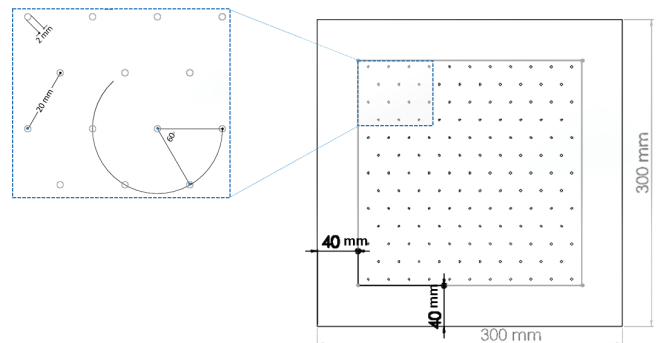


Fig. 4. Dimensioning and geometric features of the selected perforated plate.

superficial velocities. Results are shown in Fig. 5. The figure shows that the minimum pressure drop is attained at the lowest water column height of 1 cm and with 15 cm s⁻¹ air superficial velocity. Increasing water column height to 3 cm and then to 5 cm while keeping the air superficial velocity at 15 cm s⁻¹ results in a significant increase in the pressure drop. Furthermore, the air superficial velocity at 15 cm s⁻¹ is not sufficient to completely overcome the static pressure head of the 5 cm water column height such that some water leaked through the perforations. Therefore, air superficial velocity at 15 cm s⁻¹ is not taken into consideration for further investigations. The maximum pressure drop is monitored with a

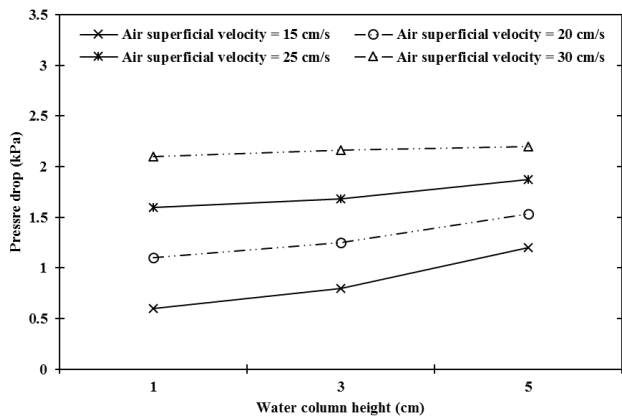


Fig. 5. Effect of water column height on the pressure drop at different air superficial velocities.

higher air superficial velocity of 30 cm s^{-1} . On contrary to the air superficial velocity of 15 cm s^{-1} , there is a slight increase in the pressure drop at higher water column heights.

The effect of water column height on the absolute humidity is also analyzed at different air superficial velocities. The humidifier is operated at 1, 3, and 5 cm water column heights. The air superficial velocity is varied from 20 to 30 cm s^{-1} for each water column height. The influence of varying air superficial velocity on the amount of vapor contents in the moist air (absolute humidity) at the exit of humidifier at different water column heights is presented in Fig. 6. The figure shows that the maximum absolute humidity is attained at the lowest water column height of 1 cm with air superficial velocity of 25 cm s^{-1} . The further increase in air superficial velocity at water column height of 1 cm slightly reduce the absolute humidity at the exit of humidifier. The reason is attributed to the short residence time of the air bubbles due to high air throughputs and air propagate very quickly from the shallow water column height of 1 cm [17]. For all other experiments performed at water column height of 3 and 5 cm, the absolute humidity is increased with the increase in air superficial velocity. The reason of attaining higher absolute humidity at higher air superficial velocity is discussed in the following section 3.2.

3.2. Influence of air superficial velocity

The investigation of varying air superficial velocity is one of the major operating parameters to optimize the performance of bubble column humidifier. As the core objective of the humidifier is to effectively humidify the air, the amount of vapor contents in the moist air (absolute humidity) at the exit of humidifier was investigated at different air superficial velocities. Fig. 7 shows that absolute humidity of air at the inlet of the humidifier, exit of the bubble column, and outlet of the humidifier at different air superficial velocities. The air is introduced to the humidifier with the help of the blower that sucks the air from the atmosphere. The absolute humidity of the inlet air is dependent on the real time atmospheric conditions and it is almost constant during the particular experimental analysis. However, the absolute humidity of the moist air at the exit of the bubble column and outlet of the humidifier is increased

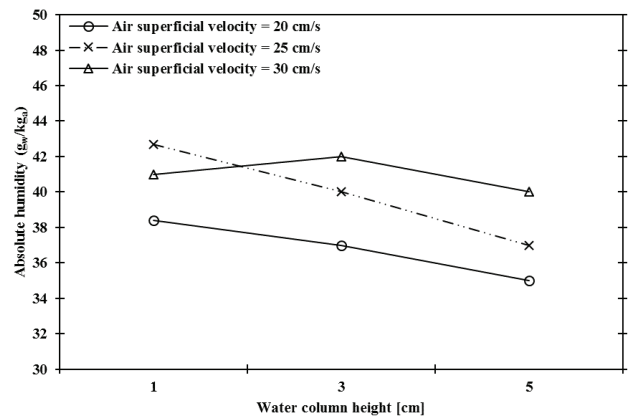


Fig. 6. Influence of water column height on absolute humidity at different air superficial velocities.

Note: Experiments were performed on 5 August, 2015 at solar irradiance of 860 W m^{-2} .

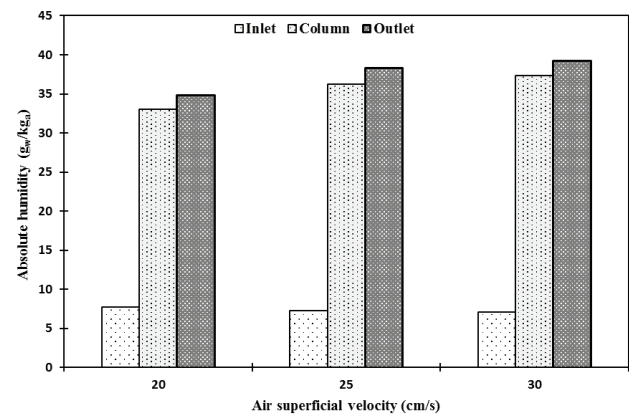


Fig. 7. Influence of air superficial velocity on the absolute humidity.

Note: Experiments were performed on 10 June, 2015 at 11 am with water column height of 3 cm. The solar irradiance value was 725 W m^{-2} .

with the increase in the air superficial velocity. The reason of attaining higher absolute humidity at higher air superficial velocity is attributed to the increased gas holdup in the bubble column. Gas holdup is a dimensionless parameter that represent the volume fraction of gas phase occupied by the bubbles. It is evident from my studies that the higher superficial velocity leads to higher gas holdup, that eventually increase the heat and mass transfer co-efficient in the bubble column [18–21]. Some studies claimed that the higher superficial velocities enhanced the turbulent motion of the of the gas bubbles and formed a disturbed homogeneous liquid-gas system with an unsteady flow pattern and large bubbles [21–24]. However, many studies revealed that the higher air superficial velocity increased the frequency of bubble formation and resulted in a mixture of small and large diameter bubbles that ranges from few millimeters to few centimeters [25,26]. The higher bubble frequency at higher air superficial velocity onsets the foam formation [27] that greatly increase the water column height during the air bubbling through the water and provide higher

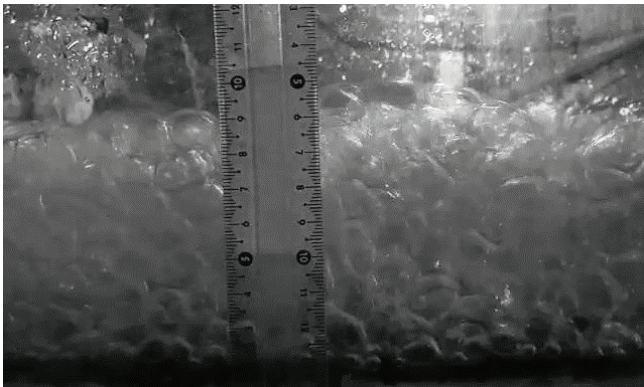


Fig. 8. Increase in water column height during air bubbling through the water at high superficial velocity.

interfacial area for better heat and mass transfer. Fig. 8 shows the process of foam formation when the water column height is maintained at 3 cm and air is sparged at superficial velocity of 30 cm s^{-1} . A large number of bubbles are formed and water column height is increased from 3 to 9 cm.

Findings also reveals that, the absolute humidity of the air significantly increases at the exit of the bubble column compared with its condition at the inlet. The significant increase in the absolute humidity is attributed to the higher rate of heat and mass transfer in the bubble column. The humid air at the exit of the bubble column further pass over the thin film of hot water flowing over the absorber plate to absorb some moisture and, consequently, the absolute humidity is further increased slightly. The slight increase in the absolute humidity is due to a lower available potential of the moist air to absorb more moisture as the moist air at the exit of the bubble column is enriched with moisture contents and close to its saturation point. The moist air approaches the water inlet temperature and leaves the humidifier almost saturated.

3.3. Influence of solar irradiance

The proposed humidifier design is novel in terms of its ability to have a direct solar thermal heating. Therefore, the performance of this humidifier design is highly influenced by the availability of the solar irradiance. Fig. 9 shows that performance of the humidifier in terms of the absolute humidity at the exit of the bubble column and the outlet of the humidifier at different solar irradiance. Results indicate that the absolute humidity of the air is increased at higher solar irradiance. Higher solar irradiance provides greater amount of the heat to the black absorber plate and increases the water temperature. The increase in the water temperature enhances the moisture absorption ability of the air and, consequently, a higher humidity ratio is achieved at the exit of the humidifier.

3.4. Influence of inlet RH

The influence of the inlet air relative humidity on the performance of the humidifier is an important aspect as it signposts the optimum performance operating conditions for its possible integration with a dehumidifier. Therefore, the performance of the humidifier is analyzed at different

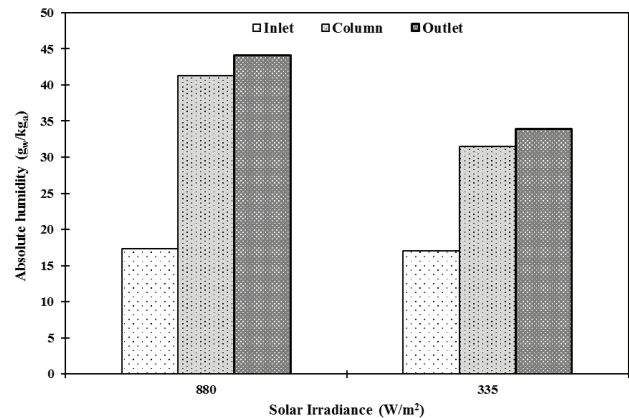


Fig. 9. Influence of solar irradiance on the absolute humidity. Note: Experiments were performed on 8 August, 2015 with water column height of 3 cm and air superficial velocity of 30 cm s^{-1} . The solar irradiance value was 890 W m^{-2} at 11 am and 440 W m^{-2} at 4 pm.

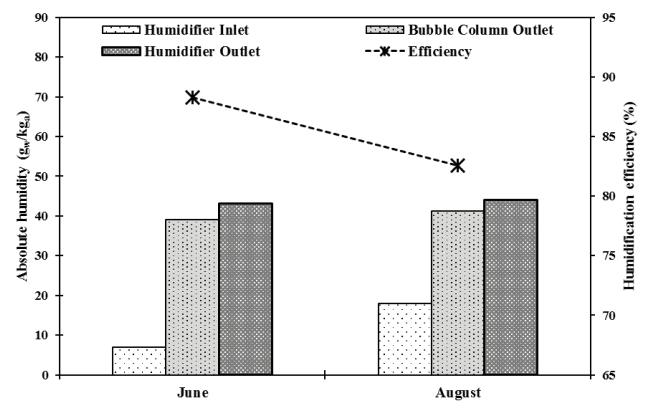


Fig. 10. Influence of relative humidity on the absolute humidity and humidification efficiency. Note: Experiments were performed on 10 June and 8 August, 2015 with water column height of 3 cm and air superficial velocity of 30 cm s^{-1} . The solar irradiance value was 890 W m^{-2} and 800 W m^{-2} at 11 am in August and June respectively.

relative humidity of the inlet air. Experiments were performed in the month of June and August to experience the climatic variations in the relative humidity of the inlet air. Fig. 10 shows that influence of inlet air relative humidity on the performance of the humidifier in terms of the humidification efficiency and the absolute humidity achieved at the exit of the humidifier. Findings reveal that the absolute humidity of the moist air at the exit of bubble column and the outlet of the humidifier is almost the same in both months of June and August. However, the humidification efficiency is higher in June compared with August. This is due to the lower relative humidity of the inlet air in the month of June compared with August. The lower relative humidity of the inlet air provides more potential to absorb moisture compared with the air with high relative humidity. This higher potential of absorbing moisture leads to a higher humidification efficiency.

3.5. Influence of water temperature

The system was operated with and without the integration of Fresnel lens between 7 am and 5 pm in June and August to analyze its performance in terms of the absolute humidity of the moist air at the exit of the humidifier. Figs. 11 and 12 show the solar irradiance on the tilted absorber plate, air and water inlet temperatures, and the water temperature achieved at the exit of absorber plate with and without the integration of Fresnel lens for particular days in June and August, respectively. It can be seen from both figures that the solar radiation and ambient air temperature rise in the morning, reach their maximum values around mid-day, and then decrease in the afternoon. Water temperature followed the same trend since it is directly influenced by the solar irradiance. The black absorber plate was heated by solar radiation. Accordingly, water temperature increases as it flows over the absorber plate. A higher water temperature

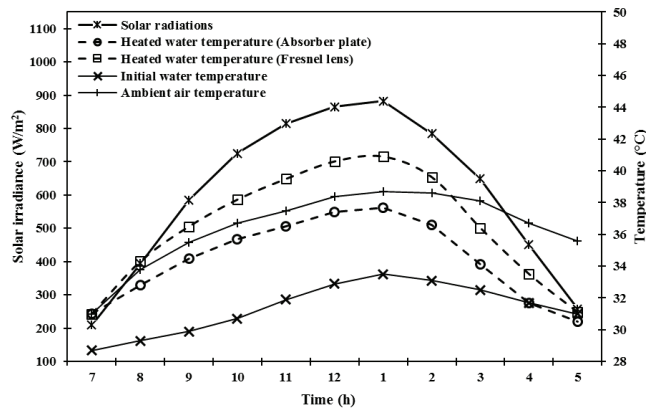


Fig. 11. Influence of solar irradiance on the water temperature in the bubble column humidifier in the month of June. Note: Data was collected at a water column height of 3 cm and air superficial velocity of 25 cm s⁻¹ on 10 June, 2015 for absorber plate experiments and on 11 June, 2015 for Fresnel lens experiments.

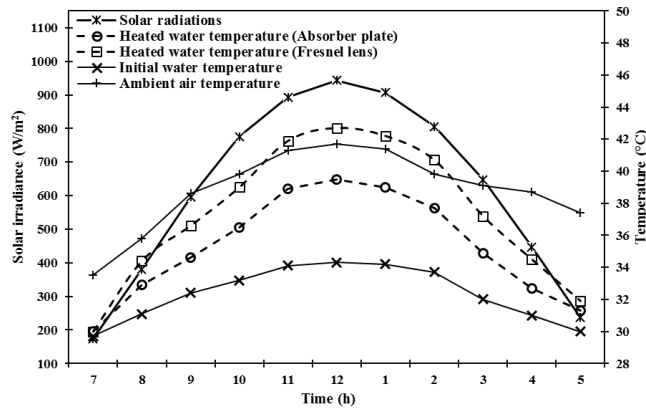


Fig. 12. Influence of solar irradiance on the water temperature in the bubble column humidifier in the month of August. Note: Data was collected at a water column height of 3 cm and air superficial velocity of 25 cm s⁻¹ on 12 August, 2015 for absorber plate experiments and on 13 August, 2015 for Fresnel lens experiments.

is achieved by using a Fresnel lens that concentrates the solar irradiance on the absorber plate and, consequently, heats the water to a higher temperature.

Since the core objective of the bubble column humidifier is to effectively humidify the air, the day round performance of the humidifier is analyzed in terms of the absolute humidity of the moist air at the exit of the humidifier. Initially, the humidifier is operated without the integration of Fresnel lens and water is heated by passing it over the absorber plate that is tilted to an angle equal to the latitude of Dhahran (26.3°), Saudi Arabia to absorb the maximum solar irradiance. Water temperature difference achieved in the humidifier and its influence on the air absolute humidity is investigated at different air superficial velocities. The investigated day round performance of the humidifier in the month of June and August is summarized in Figs. 13 and 14.

Fig. 13 shows that both the absolute humidity and the water temperature difference rise in the morning, reach their maximum values around mid-day, and then decrease in the afternoon. Results also indicate that the average day round absolute humidity is increased by 7.9% when the air superficial velocity

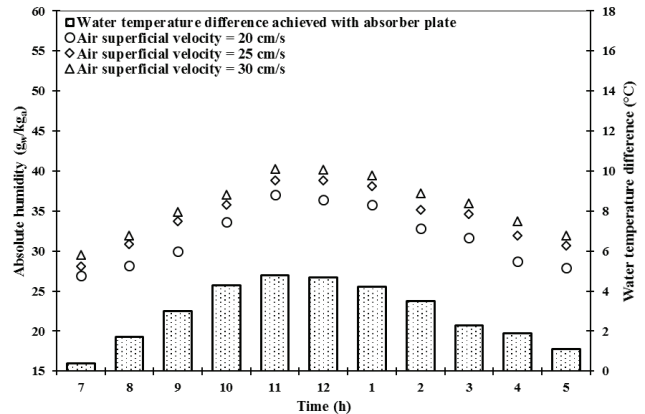


Fig. 13. Influence of water temperature and air superficial velocity on the absolute humidity of the moist air at the exit of humidifier in the month of June.

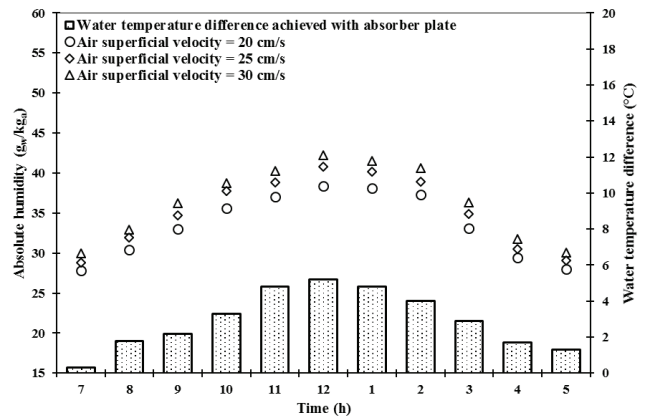


Fig. 14. Influence of water temperature and air superficial velocity on the absolute humidity of the moist air at the exit of humidifier in the month of August.

is increased from 20 to 25 cm s⁻¹. Similarly, the day round absolute humidity is further increased by 4.4% when the air superficial velocity is increased from 25 to 30 cm s⁻¹. Fig. 12 shows that similar trend with slightly different values that were caused by the variations in the climatic conditions. As the increase in water temperature enhances the ability of the air to absorb more moisture, the humidifier is integrated with Fresnel lens to achieve the higher water temperature at the inlet of bubble column humidifier. The achieved absolute humidity and water temperature difference with Fresnel lens integration in the humidifier are shown in Figs. 15 and 16 for the month of June and August, respectively. Results indicate that the average day round absolute humidity is increased in the range of 9%–11% with the integration of Fresnel lens in the humidifier for different values of the air superficial velocity. However, the integration of Fresnel lens raised the water temperature to a value that is sometimes greater than the ambient air temperature and air starts to condense on the inner surface of the glass. Although, the process of condensation is limited in the range of operating parameters and climatic conditions under which experiments were performed, this could be very common for the other

regions where the operating parameters and climatic conditions are favorable for initiating the condensation. The presence of condensed water reduces the total transmittance of solar radiations as some of the radiations are absorbed by the water layer. However, the solar absorptivity of water is very low, and the main reason for reduced transmittance is the additional reflection due to the increased roughness of the droplet-covered surface in case of drop-wise condensation. On contrary, when the condensation forms a film, the transmittance may actually be higher than that of dry glass because the refractive index of water is between that of glass and air [28]. Therefore, the use of super hydrophilic coating is one of the potential solution to tackle the issue of reduced transmission of solar radiations in the presence of condensed water as this coating encourages the film-wise condensation.

The influence of the inlet air relative humidity on the day round performance of the humidifier is investigated at different air superficial velocities. Experiments were performed in June and August to have the climatic variations in the relative humidity of the inlet air. Results are summarized in Figs. 17 and 18, respectively. Results in both figures show

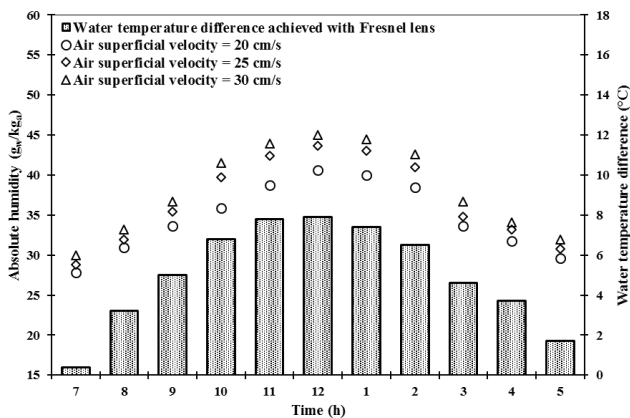


Fig. 15. Fresnel lens integration in the proposed design to increase the absolute humidity of the moist air at the exit of humidifier in the month of June.

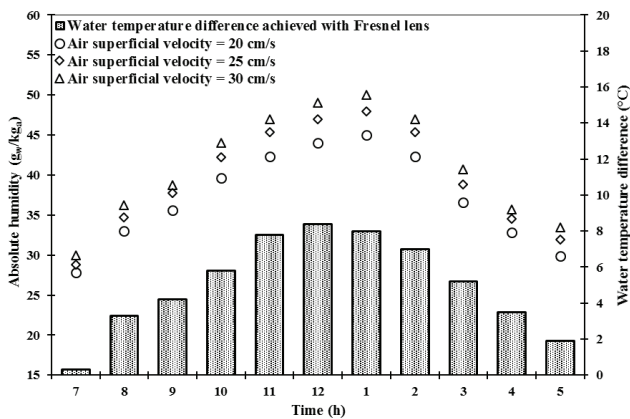


Fig. 16. Fresnel lens integration in the proposed design to increase the absolute humidity of the moist air at the exit of humidifier in the month of August.

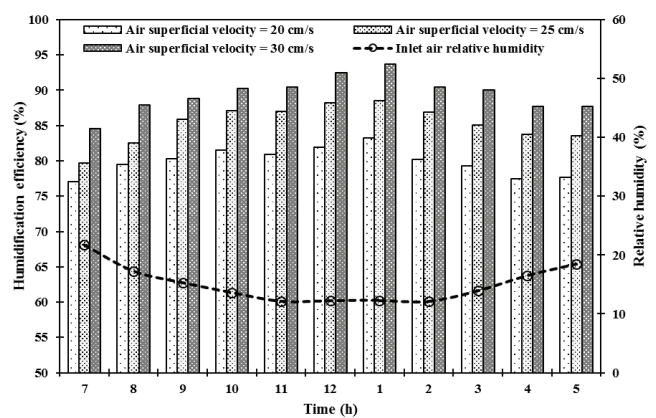


Fig. 17. Humidification efficiency of the proposed humidifier design in the month of June.

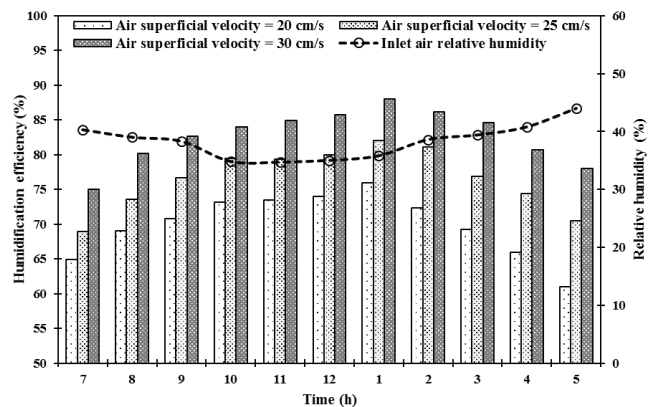


Fig. 18. Humidification efficiency of the proposed humidifier design in the month of August.

that the humidification efficiency increases with the increase in air superficial velocity irrespective of the inlet air relative humidity. However, the day round humidification efficiency of the humidifier is about 7% higher in the month of June as compared with August. This is due to the higher vapor content difference between the outlet and inlet of the humidifier in June compared with August. The reason of attaining higher vapor content difference in June is the lower relative humidity of the inlet air that varied between 12% and 22% compared with 36%–45% in August. The air at a lower relative humidity has more potential to absorb moisture compared with air at a high relative humidity.

The humidification efficiency as defined in Eq. (1) and plotted in Figs. 17 and 18 is based on the humidity difference achieved by the air between the inlet and exit of the humidifier. According to this definition, the air leaving with a higher temperature will have a higher absolute humidity that eventually will be able to produce more water. However, this performance metric is not reflecting the true performance of the solar humidifier as it does not take into account the solar energy consumed by the humidifier. Therefore, the solar humidification efficiency as defined in Eq. (2) is used to evaluate the humidifier performance. Fig. 19 shows that day round solar humidification efficiency of the humidifier. The experiments were performed in the month of June with and without the integration of Fresnel lens. The solar humidification efficiency achieved with and without the integration of Fresnel lens is presented as Fresnel lens case and absorber plate case, respectively. Results demonstrate that the solar humidification efficiency in absorber plate case varies with in the range of 70%–80% during its day-round operation. However, the solar humidification efficiency is comparatively very low in Fresnel lens case and varies with in the range of 30%–42% during its day-round operation. The lower value of solar humidification efficiency in Fresnel lens case is attributed to the low efficiency of the Fresnel lens. Although, the Fresnel lens integration concentrate the solar radiations on the absorber plate and helped in achieving the higher temperature at the downstream of the absorber plate, the amount of solar radiations concentrated on the absorber plate is much lower than the amount of solar radiations incident on the Fresnel lens. This is due to the fabrication errors of the commercially available Fresnel lens due to which the incident solar radiations on the lens suffer from 30% to 40% losses before these radiations are concentrated on the absorber plate [29].

Fig. 20 shows the day round solar humidification efficiency of the humidifier in the month of August with and without the integration of Fresnel lens. Although the solar irradiance, inlet water temperature, and ambient air temperature is almost same in the month of June and August (as shown in Figs. 11 and 12), Fig. 20 demonstrate a comparatively lower solar humidification efficiency in the month of August that varies with in the range of 40%–50% for absorber plate case and 20%–30% for Fresnel lens case. The lower solar humidification efficiency is due to the higher relative humidity of the inlet air in the month of August. The specific enthalpy of the inlet air is higher due to the higher inlet air relative humidity and the air at the exit of the humidifier achieve lower enthalpy difference between the inlet and exit state of the humidifier. Consequently, the air between the inlet and exit state gain less energy as compared with the

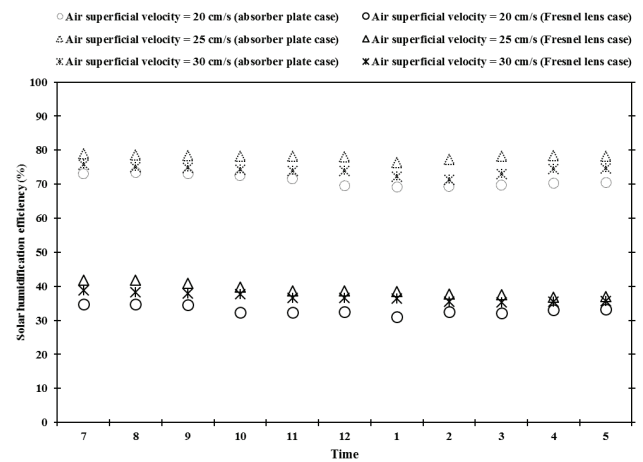


Fig. 19. Solar humidifier efficiency at various air superficial velocities in the month of June with and without the integration of Fresnel lens.

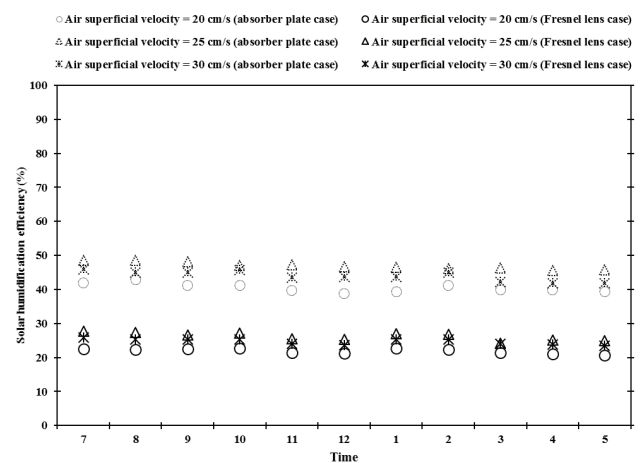


Fig. 20. Solar humidifier efficiency at various air superficial velocities in the month of August with and without the integration of Fresnel lens.

humidifier operated in the month of June. Hence, the system shows lower solar humidification efficiency in the climatic conditions that have a higher inlet air relative humidity.

4. Conclusions

In this study, a novel bubble column humidifier was developed and tested to identify the optimum performance operating conditions for its possible integration with a dehumidifier. Different design configurations of the perforated plate were tested in order to achieve the lower pressure drop in the system. Findings revealed that the minimum pressure drop was experienced at a lower water column height and a lower air superficial velocity. However, the water column height and the air superficial velocity should be optimized according to the geometry of the perforated plate in order to avoid water leakage through the perforations.

The performance of the humidifier in terms of air absolute humidity at the exit of the humidifier is increased by increasing the air superficial velocity and water temperature. The humidifier was integrated with the Fresnel lens in order to achieve a higher water temperature. The increase in water temperature enhanced the ability of air to absorb more moisture and consequently higher absolute humidity is achieved at the outlet of the humidifier. However, due to the non-ideal nature of the commercially available Fresnel lens, the amount of solar radiations concentrated on the absorber plate is much lower than the amount of solar radiations incident on the Fresnel lens. Therefore, the solar energy based humidification efficiency of the Fresnel lens integrated humidifier is much lower as compared with the humidifier operated without the integration of Fresnel lens. Moreover, the humidifier performs better in the climatic conditions that have a lower inlet air relative humidity.

Symbols

$c_{p,a}$	— Specific heat capacity of air, $\text{kJ kg}^{-1} \text{ } ^\circ\text{C}^{-1}$
$c_{p,w}$	— Specific heat capacity of water, kJ kg^{-1}
h_a	— Specific enthalpy of moist air, kJ kg^{-1}
$h_{a,i}$	— Specific enthalpy of moist air at the inlet of humidifier, kJ kg^{-1}
$h_{a,o}$	— Specific enthalpy of moist air at the outlet of humidifier, kJ kg^{-1}
h_{da}	— Specific enthalpy of dry air, kJ kg^{-1}
h_{wv}	— Specific enthalpy of water vapor, kJ kg^{-1}
$h_{e,w}$	— Evaporation heat of water, kJ kg^{-1}
$\dot{m}_{a,i}$	— Mass flow rate of air at the inlet of humidifier, Kg s^{-1}
$\dot{m}_{a,o}$	— Mass flow rate of air at the outlet of humidifier, Kg s^{-1}
Q_{solar}	— Solar energy incident on the humidifier, J s^{-1}
T_a	— Temperature of air, $^\circ\text{C}$
T_w	— Temperature of water, $^\circ\text{C}$
ω_{in}	— Absolute humidity of the air at the inlet of humidifier, $\text{g}_w \text{ kg}_a^{-1}$
ω_{out}	— Absolute humidity of the air at the outlet of humidifier, $\text{g}_w \text{ kg}_a^{-1}$
$\omega_{\text{out}}^{\text{sat}}$	— Saturated absolute humidity of the air at the outlet of humidifier, $\text{g}_w \text{ kg}_a^{-1}$
x	— Humidity ratio, kg kg^{-1}

Acknowledgments

The authors acknowledge the support of King Fahd University of Petroleum and Minerals (KFUPM), Dhahran, Saudi Arabia for this work through project number IN131041 and the support of the Center of Research Excellence in Renewable Energy, KFUPM, Dhahran, Saudi Arabia.

References

- [1] H.M. Abd-ur-Rehman, F.A. Al-Sulaiman, Optimum selection of solar water heating (SWH) systems based on their comparative techno-economic feasibility study for the domestic sector of Saudi Arabia, *Renew. Sustain. Energy Rev.*, 62 (2016) 336–349.
- [2] Y. Liu, Y. Guo, Q. Wei, Analysis and evaluation of various energy technologies in seawater desalination, *Desal. Water Treat.*, 51 (2013) 3743–3753.
- [3] D.S. Likhachev, F.C. Li, Large-scale water desalination methods: a review and new perspectives, *Desal. Water Treat.*, 51 (2013) 2836–2849.
- [4] M. Moser, F. Trieb, T. Fichter, J. Kern, Renewable desalination: a methodology for cost comparison, *Desal. Water Treat.*, 51 (2013) 1171–1189.
- [5] M.A. Darwish, H.K. Abdulrahim, A.S. Hassan, A.A. Mabrouk, PV and CSP solar technologies and desalination: economic analysis, *Desal. Water Treat.*, 57 (2016) 16679–16702.
- [6] A.E. Kabeel, E.M. El-Said, Development strategies and solar thermal energy utilization for water desalination systems in remote regions: a review, *Desal. Water Treat.*, 52 (2014) 4053–4070.
- [7] G.P. Narayan, J.H. Lienhard, Thermal design of humidification–dehumidification systems for affordable small-scale desalination, *IDA J. Desal. Water Reuse*, 4 (2012) 24–34.
- [8] W. Abdelmoez, M.S. Mahmoud, T.E. Farrag, Water desalination using humidification/dehumidification (HDH) technique powered by solar energy: a detailed review, *Desal. Water Treat.*, 52 (2014) 4622–4640.
- [9] R.E. Treybal, *Mass Transfer Operation*, McGraw-Hill, New York, 1980.
- [10] S. Degaleesan, M. Dudukovic, Y. Pan, Experimental study of gas-induced liquid-flow structures in bubble columns, *AIChE J.*, 47 (2001) 1913–1931.
- [11] S.A. El-Agouz, M. Abugderah, Experimental analysis of humidification process by air passing through seawater, *Energy Convers. Manage.*, 49 (2008) 3698–3703.
- [12] S.A. El-Agouz, Desalination based on humidification–dehumidification by air bubbles passing through brackish water, *Chem. Eng. J.*, 165 (2010) 413–419.
- [13] S.A. El-Agouz, A new process of desalination by air passing through seawater based on humidification–dehumidification process, *Energy*, 35 (2010) 5108–5114.
- [14] L. Zhang, S. Gao, H. Zhang, Experimental Researches of Factors Affecting Bubbling Humidification, *Advances in Computer Science, Intelligent System and Environment*, Springer Berlin Heidelberg, 2011, pp. 359–364.
- [15] L. Zhang, G. Cheng, S. Gao, Experimental study on air bubbling humidification, *Desal. Water Treat.*, 29 (2011) 258–263.
- [16] N.C. Barford, J.W. Richards, J.B. Kelley, Experimental measurements: precision, error and truth and interpretation of technical data, *Phys. Today*, 22 (2009) 109–111.
- [17] N. Kantarci, F. Borak, K.O. Ulgen, Bubble column reactors, *Process Biochem.*, 40 (2005) 2263–2283.
- [18] Y.T. Shah, B.G. Kelkar, S.P. Godbole, W.D. Deckwer, Design parameters estimations for bubble column reactor, *AIChE J.*, 28 (1982) 353–379.
- [19] R. Krishna, J.W. De Swart, J. Ellenberger, G.B. Martina, C. Maretto, Gas holdup in slurry bubble columns: effect of column diameter and slurry concentrations, *AIChE J.*, 43 (1997) 311–316.
- [20] J.G. Daly, S.A. Patel, D.B. Bukur, Measurement of gas holdups and sauter mean bubble diameters in bubble column reactors by dynamics gas disengagement method, *Chem. Eng. Sci.*, 47 (1992) 3647–3654.
- [21] H. Li, A. Prakash, Influence of slurry concentrations on bubble population and their rise velocities in a three-phase slurry bubble column, *Powder Technol.*, 113 (2000) 158–167.
- [22] M. Fukuma, K. Muroyama, S. Morooka, Properties of bubble swarm in a slurry bubble column, *J. Chem. Eng. Jpn.*, 20 (1987) 28–33.
- [23] S.C. Saxena, N.S. Rao, A.C. Saxena, Heat-transfer and gas-holdup studies in a bubble column: air–water–glass bead system, *Chem. Eng. Commun.*, 96 (1990) 31–55.
- [24] C.L. Hyndma, F. Larachi, C. Guy, Understanding gas-phase hydro-dynamics in bubble columns: a convective model based on kinetic theory, *Chem. Eng. Sci.*, 52 (1997) 63–77.
- [25] A. Matsuura, L.S. Fan, Distribution of bubble properties in a gas–liquid–solid fluidized bed, *AIChE J.*, 30 (1984) 894–903.
- [26] W. Li, W. Zhong, B. Jin, R. Xiao, Y. Lu, T. He, Study of the particle size effect on bubble rise velocities in a three-phase bubble column, *Int. J. Chem. Nucl. Mater. Metall. Eng.*, 7 (2013) 609–613.
- [27] L. Pilon, R. Viskanta, Minimum superficial gas velocity for onset of foaming, *Chem. Eng. Process.*, 43 (2004) 149–160.
- [28] E.W. Tow, The antireflective potential of dropwise condensation, *J. Opt. Soc. Am. A.*, 31 (2014) 493–499.
- [29] M.S. Mahmoud, T.E. Farrag, W.A. Mohamed, Experimental and theoretical model of water desalination by humidification–dehumidification (HDH), *Procedia Environ. Sci.*, 17 (2013) 503–512.